Environmental Earth Sciences (2025) 84:382
https://doi.org/10.1007/s12665-025-12391-1

ORIGINAL ARTICLE

Future changes in drought characteristics in the Central Black Sea region of Türkiye using HadGEM2-ES climate models and the SPI

Selcuk Erdem Kurtoglu[1] · Aslı Ulke Keskin[1] · Utku Zeybekoglu[2]

Received: 27 January 2025 / Accepted: 14 June 2025 / Published online: 25 June 2025

Abstract
This study investigates future changes in meteorological drought characteristics in the Central Black Sea Region of Türkiye (Tokat, Çorum, Amasya, Ordu, and Samsun) for the period 2023–2080. Using precipitation projections from the HadGEM2-ES climate model under RCP4.5 and RCP8.5 scenarios, the Standardized Precipitation Index (SPI) was applied at 1-, 3-, 6-, and 12-month timescales. The analysis reveals a reduction in the frequency of near-normal wet conditions, alongside a noticeable increase in the frequency and severity of dry periods, particularly in the inland provinces. Although some coastal areas are projected to receive more precipitation, drought conditions are still expected to intensify, reflecting complex regional responses to climate change. The results of this study are intended to support long-term water resource management, agricultural planning, and climate adaptation efforts in the region.

Keywords Climate change · GCM · Projection · Precipitation

Introduction

Climate change, defined by the UNFCCC as a long-term alteration in atmospheric composition due to human and natural factors, is increasingly viewed through the lens of anthropogenic impact (UNFCCC 1992). While some scholars assert that climate variability has accompanied humanity throughout history, others emphasize its intensification with modernity and the Industrial Revolution (Ekici 2022). According to the IPCC's Fifth Assessment Report, global warming is unequivocal, and post-1950 climate anomalies are unprecedented in the last millennium (Turkes 2020). The Sixth Assessment Report further attributes 95% of climate change to human activities (IPCC 2021), highlighting several key indicators: a global temperature increase of 1.07 °C from 1850–1900 to 2010–2019, Arctic sea ice and Northern Hemisphere snow cover loss, surface melt of the Greenland Ice Sheet, reduction of Antarctic ice, ocean warming and acidification, a 0.20 m sea level rise between 1901 and 2018, and atmospheric CO_2 levels exceeding those of the past two million years. It also notes more frequent extreme weather events, changing monsoon patterns, and a rise in tropical cyclone activity. These phenomena are all linked to human-induced radiative forcing and increased surface warming (IPCC 2021; Turkes 2022). Additionally, WMO data identify 2021 as among the seven hottest years recorded, reflecting sustained industrial-era warming. This shift disrupts seasonal patterns—shortening winters, extending summers, and threatening ecosystems as species struggle to adapt. The redistribution of tropical zones, shifts in water and agricultural regions, and marine acidification further illustrate the multifaceted consequences of climate change, including heightened risks of erosion, flooding, and desertification (Ilkkilic 2022).

Heinrich and Gobiet (2012) used RCM simulations from the ENSEMBLES project to analyze drought and wet period characteristics across nine European locations for 2021–2050, based on 1961–1990 observations. They found pronounced extremes in duration, magnitude, and spatial extent, especially in southern (France, Italy, Spain) and northern (Iceland, Scandinavia) regions, with significantly

✉ Utku Zeybekoglu
utkuz@sinop.edu.tr

Selcuk Erdem Kurtoglu
s.erdemkurtoglu@hotmail.com

Aslı Ulke Keskin
asli.ulke@omu.edu.tr

1 Faculty of Engineering, Ondokuz May University, 55139 Atakum, Samsun, Türkiye

2 Boyabat Vocational School of Higher Education, Sinop University, 57200 Boyabat, Sinop, Türkiye

increased interannual variability in wetter and drier areas. Sienz et al. (2012) compared the reliability of gamma distributions (GD) for monthly precipitation using Weibull (WD), Burr Type III (BD), exponentiated Weibull (EWD), and generalized gamma (GGD) distributions, based on data from 1901–2002 and simulations for 2001–2100 in England-Wales. The study found that WD provided the most consistent and accurate distribution compared to GD, as assessed using the Akaike information criterion (AIC). Mo and Lyon (2015) analyzed precipitation data from North America (1950–2010) using various models (NMME, NCEP, GFDL, NCAR, NASA, CMC1, CMC2). They highlighted the importance of the proximity of SPI forecasts to actual precipitation data, considering it a significant advancement for the Global Drought Information System (GDIS). Duffy et al. (2015) project increased drought frequency in the eastern Amazon and more extreme wetness after 2040 under the RCP8.5 scenario. Severe droughts could triple by 2100, posing risks to Amazonian forests.

Stagge et al. (2015) projected future drought scenarios in Europe using RCP2.6, RCP4.5, and RCP8.5 models for 1970–2005 and three future periods (2011–2040, 2041–2070, 2071–2100) with the CORDEX method. They analyzed the data using statistical tests (Welch, Kolmogorov–Smirnov, and Chi-square) to assess model accuracy and emphasized the importance of selecting the best climate model for effective drought mitigation strategies in Europe. Choi et al. (2016), project future droughts in South Korea using five RCMs under RCP4.5 and RCP8.5 scenarios. Droughts, measured with SPI-1, SPI-6, and SPI-12, show variable trends. The number of drought months increases under RCP8.5 (2041–2070) and RCP4.5 (2071–2100). Overall, drought-affected areas are projected to decrease, except for SPI-1 under RCP4.5, which shows a slight increase. Diaconescu et al. (2016) analyzed observed precipitation data (1989–2004) in North America using SPI and simulations from the Canadian regional models CANRCM4 and CRCM5. The study compared these simulations with previous Canadian RCMs and those in NARCCAP, finding that CRCM4 performed best according to NCEP-R2 scores. The CRCM5 model, however, was better at simulating Eastern U.S. states, particularly excelling in winter and improving summer forecasts significantly. Dabanli et al. (2017) analyze drought variability in Türkiye (1931–2010) using SPI indices and PCA. The study identifies four drought-vulnerable regions and calculates the percentage of extreme, severe, and moderate droughts. Southeastern and western Türkiye are more stable, while central and northern regions are less stable. The impact of ENSO phases on droughts is also discussed.

Agyekum et al. (2018) examined seasonal timelines and the differences between observed and modeled precipitation for 1950–2004 in the Volta Basin, Gulf of Guinea, using 18 global climate models (GCMs) from the Coupled Model Intercomparison Project Phase 5 (CMIP5). The study found that the CCSM4 model was the most successful in simulating precipitation patterns. Demory et al. (2020) evaluated precipitation distributions in Europe (1971–2005) using global climate models (GCM) from the High-Resolution Model Intercomparison Project (HighResMIP), EURO-CORDEX, and regional climate models (RCM) developed under the EU-funded PRIMEVERA initiative. The study found that PRIMAVERA simulations closely matched observed heavy precipitation in most regions and seasons, whereas CORDEX tended to overestimate extreme rainfall. However, both models were deemed reliable, depending on the variable parameters. Danandeh Mehr et al. (2020) analyzed drought in Ankara for 2016–2040 using SPI and SPEI with three climate models under RCP4.5 and RCP8.5 scenarios. Results suggest that under RCP4.5, drought events are likely in the latter half of the period, whereas under RCP8.5, drought conditions are expected throughout the entire timeframe. Afshar et al. (2020) assess climate change impacts on droughts in Ankara, Türkiye, using rainfall data and climate model outputs under RCP 4.5 and RCP 8.5. They find increased drought occurrence, longer durations, and greater severity in the future. Extreme droughts are projected to occur more frequently, with a 12% decrease in the return period. Nuri Balov and Altunkaynak (2020) assessed future drought trends in Türkiye's Western Black Sea and Euphrates-Tigris basins using SPI, Chinese Z Index, and Statistical Z Score under three climate models. Projections for 2040–2069 and 2070–2099 indicate increasing drought duration and intensity, especially under RCP8.5. All indices showed consistent spatial and temporal patterns.

Wood et al. (2021) conducted a global study using six climate models (CanESM2, CSIRO, GFDL-ESM2M, CESM, GFDL-CM3, MPI) as part of the SMILE project, analyzing observational data from the Frogs database (1950–2016). Their findings indicated that the CESM and MPI models optimally capture interannual precipitation variability across most global land areas. Secci et al. (2021) analyzed groundwater responses in Northern Tuscany using SPI, SPEI, and SGI based on historical precipitation and well data. Regression models under RCP4.5 and RCP8.5 scenarios project widespread future declines in groundwater levels. The greatest reduction is expected in the medium term under RCP4.5, and in the long term under RCP8.5. Salimian et al. (2021) applied LARS, IHACRES, and Bayesian models to 14 selected climate projections in the Karkheh Basin, Iran, using standardized precipitation and flow indices. Projections for 2020–2049 indicate a 54% probability of near-normal drought conditions in the region. Xu et al. (2023) projected global drought conditions from 2016 to 2100 using CMIP6 data and the daily SPEI algorithm. Their findings show that droughts will become more severe globally, with regional variations, and precipitation is the main driver of drought events. Montes-Vega et al. (2023) used SPI, SPEI, and GRDI methods with RCP4.5 and RCP8.5 scenarios to project climate trends in Doñana National Park for 2030–2060. Their model indicates significant temperature increases and a 13–14% reduction in total precipitation, with heavy rainfall events declining by 25–38%. Average annual precipitation is projected to drop from 575 to 496 mm (RCP4.5) and 493 mm (RCP8.5). Moutia and Sinan (2024) projected drought trends in Morocco for the period 2023–2099 using the CMIP6 climate model under the SSP2-4.5 scenario, based on the Standardized Precipitation Evapotranspiration Index (SPEI). Their findings indicate a progressive expansion of moderate drought conditions nationwide, with a decadal increase of approximately 6%. Furthermore, the study anticipates the emergence of severe drought events in the latter half of the century. Taylan (2024) forecasts droughts in the Sakarya Basin (2024–2034) using SPI and LSTM methods. The study validates LSTM's accuracy in predicting droughts and creates drought maps to identify vulnerable areas, aiding long-term water resource planning and drought management. Rayhan and Afraz (2024) compared five bias-corrected RCMs for the Western region of Bangladesh and found that the MIROC model had the highest accuracy. Future projections under the RCM 8.5 W/m^2 scenario suggest that short-term droughts (SPI-3) will become less frequent and severe by the 2060 s and 2080 s, with the North-West region remaining more drought-prone than the South-West until 2100.

Sen and Sisman (2024) highlight the difference between the probabilistic standardization index (PSI) and statistical standardization procedure (SSP) in the Standardized Precipitation Index (SPI). They explain that PSI correctly transforms hydro-meteorological data to a standard Gaussian distribution, while SSP does not. The study compares PSI and SSP, demonstrating the proper use of PSI with data from the Danube, New Jersey, and Istanbul. Abu Arra and Sisman (2024a) propose a drought classification matrix for comparing drought indices and scenarios, addressing gaps in traditional methods. Applied to stations in the UK and Türkiye, their study finds that a 10-year period is sufficient for meteorological drought, while a 20-year period is needed for hydrological drought, providing a robust framework for global drought assessments. Abu Arra et al. (2024) developed the Periodic Innovative Polygon Trend Analysis (P-IPTA) method to analyze seasonal effects on hydro-meteorological series at various temporal scales. Applied to precipitation, water availability (Istanbul), and stream flow (Danube River), the method revealed decreasing trends, increased drought frequencies, and reduced wet event frequencies. P-IPTA, along with traditional methods like SPI, SPEI, and SDI, provides more reliable results and can be applied to a wide range of variables. Korkmaz and Kuriqi (2024) analyze drought conditions in Tunceli, Türkiye, using multiple indices (SPI, RDI, PNI, AI). The study finds that the region is shifting from humid to semi-arid, with RDI showing less variation than SPI. These findings stress the need for climate adaptation strategies and sustainable water management. Abu Arra and Sisman (2024b) compared SPI and SPEI using the innovative drought classification matrix (IDCM) for Istanbul (1951–2020). The study found a high correlation (over 0.65) between the two indices, with 60% consistency in monthly drought classifications. Significant differences were found between in situ and satellite-based SPEI. This comparison is essential for accurate drought assessment and water resources management. Türkiye is expected to be significantly affected by climate change. Climate projections based on RCP4.5 and RCP8.5 scenarios estimate an annual average temperature increase of 1 °C to 5 °C between 2016 and 2099 (Demircan et al. 2017). According to the IPCC Sixth Assessment Report, warming in Türkiye may exceed global averages by 40–50%, with Southeastern Anatolia surpassing the global mean even in a 1.5 °C scenario (IPCC 2021).

The objective of this study is to examine the potential drought conditions in the Central Black Sea region, which, despite its high precipitation, is vulnerable to drought for the period 2023–2080. This investigation employs the SPI and HadGEM2-ES (RCP4.5 and RCP8.5) climate models to analyze the anticipated drought situation. Consequently, this study will ascertain the future impact of drought in the region under investigation. Moreover, to the best of the authors' knowledge, there is no study examining the future drought situation of the Central Black Sea Region within the scope of climate projections. Kurtoglu (2024) examined the precipitation data from Turkish State Meteorological Service (TSMS) stations in the Central Black Sea Region for the period 2018–2022 and compared it with the precipitation outputs from three different climate models (HadGEM2-ES, MPI-ESM-MR, GFDL-ESM2M). The analysis revealed that the HadGEM2-ES model showed the closest match to the observed precipitation values. As a result, Kurtoglu (2024) recommended the HadGEM2-ES model as the most reliable option for future projections. The article is divided into five sections. Section "Introduction" provides a comprehensive overview of the study's objectives, underpinned by a meticulous examination of extant literature. Section "Materials and methodology" of the article provides a comprehensive overview of the study area, the data sources, and the analytical method employed in the study. Section "Results" and Section "Discussion" of this article is concerned with the evaluation of the findings obtained as a result of the analyses. The final section of the article presents the conclusion.

Materials and methodology

Study area

The Central Black Sea Region between 35°- 38° east longitude and 40°- 42° north latitude covering the Tokat, Çorum, Amasya, Ordu, and Samsun in Türkiye was determined as the study area. Samsun and Ordu are located on the Black Sea coast, while Tokat, Amasya, and Çorum are located inland. The Central Black Sea Region is located in the central part of the Black Sea Region. The Central Black Sea Region has a temperate climate. Day-night temperature differences are less than in continental climate zones. Samsun and Ordu receive more precipitation than Tokat, Amasya, and Çorum, which are located in the transition region, and average precipitation values are between 545 and 1946 mm. The highest temperatures in these stations are between 29° and 40.5℃ and the lowest temperatures are between 0° and −22℃. The average daily temperatures are between 5° and 15 °C. In Tokat, Amasya, and Çorum, which are located in the transition zone, the average precipitation is 252–808 mm and the highest temperature values are 28°- 45 °C. The lowest temperatures in these stations are between −27.3° and −8.7 °C, and their average daily temperatures are between 6° and 15 °C (Kiciman 2021).

The dataset used in this study included precipitation series recorded at 5 stations by the TSMS in the Black Sea Region of Türkiye. The localization of Samsun, Ordu, Amasya, Tokat, and Çorum meteorological stations used in the study in the region is given in Fig. 1 and positional and numerical details (1971–2022) are given in Table 1.

Global climate models

Global climate models play a vital role in defining global climate statistics, such as global mean surface temperature. GCMs are models which represent physical processes in the atmosphere, oceans, cryosphere and land surface. These models represent the most sophisticated tools available for demonstrating the response of the climate system to rising greenhouse gas emissions. The utilisation of regional climate models facilitates the development of higher-resolution climate projections through the integration of low-resolution

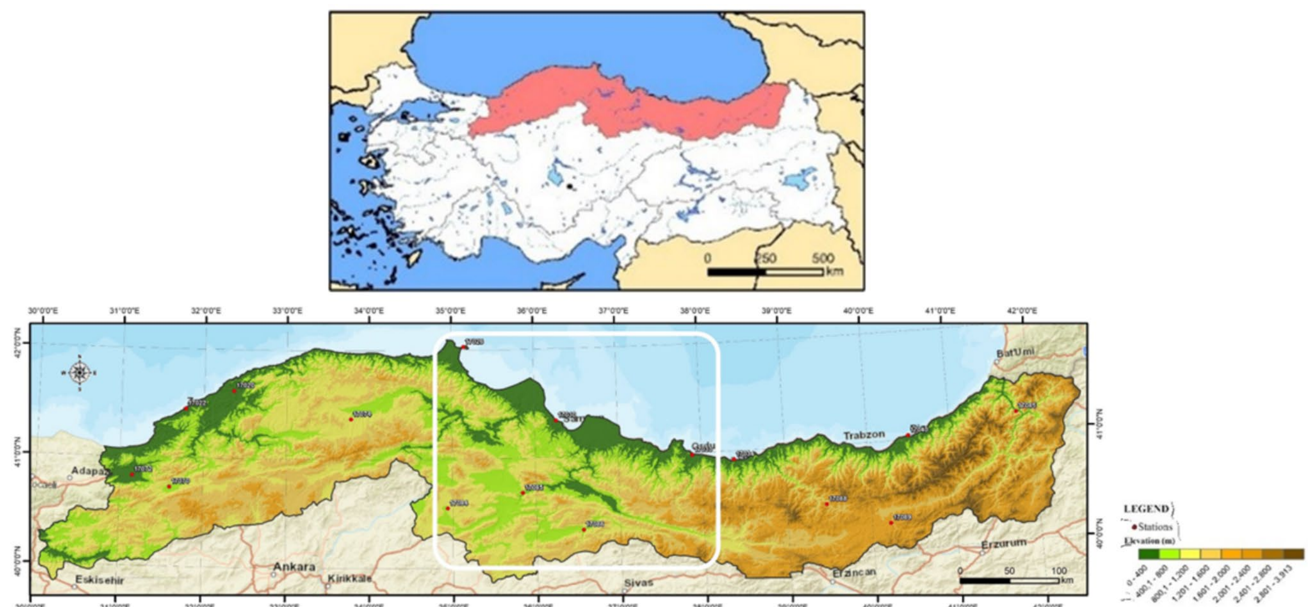

Fig. 1 Distribution of stations in the Central Black Sea Region

Table 1 Positional characteristics and meteorological details (monthly) of stations

ID	Station	Altitude (m)	Latitude (°N)	Longitude (°E)	Mean (mm)	Median (mm)	Max. (mm)
17085	Amasya	409	40.5786	35.868	37.90	32.80	153.90
17084	Çorum	776	40.6284	34.8927	37.33	31.40	220.10
17033	Ordu	5	40.8213	37.861	87.70	79.15	267.60
17030	Samsun	4	41.3051	36.187	58.91	52.10	269.80
17086	Tokat	611	40.3504	36.5784	36.05	32.30	141.10

Global Climate Model data, employing a range of methodologies (Yildirim and Gurkan 2016).

HadGEM2-ES is a second-generation global model developed by the Hadley Centre, a research organisation affiliated with the Met Office. Notably, there are numerous versions of this model, which possess analogous physical properties but divergent structures. The HadGEM2 series encompasses a coupled atmosphere–ocean configuration and a land-system configuration, incorporating dynamic vegetation, ocean biology, and atmospheric chemistry. The HadGEM2 series is one of the models utilised in the preparation of the IPCC 5th Report. The HadGEM2 series encompasses the following versions: HadGEM2-A, HadGEM2-O, HadGEM2AO, HadGEM2-CC, HadGEM2-CCS, and HadGEM2-ES (Collins et al. 2008; TSMS 2015). It is evident that HadGEM2-ES represents a more advanced model in comparison to its other versions (TSMS 2015). MPI-ESM-MR is a new generation Earth System Model (ESM) developed by the Max Planck Institute for Meteorology in Hamburg, Germany, following a five-year research project that utilised the European Central Hamburg Model (ECHAM5) atmospheric model and MPIOM ocean general circulation models. Three distinct versions of the model have been developed: MPI-ESM-LR, MPI-ESM-MR and MPI-ESM-P as LR (Giorgetta et al. 2012; TSMS 2015). The MPI-ESM-MR version provides a more detailed representation of the atmospheric layers than the other two versions (TSMS 2015). GFDL-ESM2M is a global Earth System Model developed by the Geophysical Fluid Dynamics Laboratory (GFDL) of the National Oceanic and Atmospheric Administration (NOAA). GFDL is a unified global climate model that examines the interaction of material cycles (carbon, water, etc.) on the Earth and human activities on climate systems. During the development of the model, studies were conducted to best demonstrate the interactions between climate and ecosystem and the changes that may occur in these due to both natural and human-induced causes. Two versions are in existence: GFDL-ESM2M and GFDL-ESM2G (Delworth et al. 2006; Dunne et al. 2012, 2013; TSMS 2015). The final report of the project, prepared by the TSMS and published in 2015 under the title "Türkiye Climate Projections and Climate Change with New Scenarios TR2015-CC", presents the results of climate projections for Türkiye. These projections were developed using the RegCM4.3.4 regional climate model, which was based on data from the HadGEM2-ES, MPI-ESM-MR and GFDL-ESM2M global climate models, as well as the RCP4.5 and RCP8.5 scenarios. In the study, the reference period was selected as 1971–2000, and climate projections were produced for the future period up to 2100 (TSMS 2015; Yildirim and Gurkan 2016).

Kurtoglu (2024) conducted a comparison between the precipitation data collected from stations in the Central Black Sea Region by TSMS between 2018 and 2022 and the precipitation values produced by three different climate models. After a comprehensive assessment, it was found that the HadGEM2-ES model aligned more closely with the observed precipitation values. As a result, Kurtoglu (2024) recommended the HadGEM2-ES model as the most suitable option.

Standardized precipitation index (SPI)

McKee et al. (1993) developed the Standardized Precipitation Index (SPI) to identify and monitor regional drought conditions. SPI enables the standardized transformation of observed precipitation data into probability-based values and can be calculated over various time scales, including 1, 3, 6, 9, 12, 24, and 48 months. Short-term time scales (weekly and monthly) are particularly relevant for assessing agricultural water needs and water availability, while long-term periods (12, 24, or 36 months) are crucial for water supply planning, water resource management, and groundwater studies (Mishra and Desai 2005; Mishra and Singh 2011). SPI can be computed based on several precipitation probability distributions, including the normal, log-normal, and gamma distributions (Yacoub and Tayfur 2017). However, numerous studies have reported that climatic precipitation series generally fit the gamma distribution more accurately (Thom 1958; Mishra and Desai 2005; Mishra and Singh 2010; Yacoub and Tayfur 2017). The probability density function of the gamma distribution, (x), is expressed as:

$$g(x) = \frac{1}{\beta^{\alpha}\Gamma(\alpha)} x^{\alpha-1} e^{-x/\beta} \tag{1}$$

and the gamma probability density function is given as:

$$\Gamma(\alpha) = \int_0^{\infty} x^{\alpha-1} e^{-y} dx \tag{2}$$

where x represents the amount of precipitation, $\Gamma(\alpha)$ is the gamma function, and α and β are the shape and scale parameters, respectively. To compute the SPI, a gamma probability density function must be fitted to the frequency distribution of precipitation totals recorded at a given station. The shape (α) and scale (β) parameters of the gamma distribution are estimated individually for each station and for each relevant time scale. The maximum likelihood estimation method proposed by Thom (1958) is commonly employed to derive these parameters (Bacanli et al. 2009; Bacanli and Kargi 2019). The shape and scale parameters are calculated as follows:

$$\alpha = \frac{1}{4A}\left(1 + \sqrt{1 + \frac{4A}{3}}\right); \beta = \frac{\overline{x}}{\alpha}; A = ln(\overline{x}) - \sum \frac{ln(x)}{n} \tag{3}$$

where n denotes the number of observations. The estimated parameters are then utilized to construct the cumulative probability function (*x*), which is defined by the following expression (Bacanli 2017):

$$G(x) = \int_0^x g(x)dx = \frac{1}{\beta^\alpha \Gamma(\alpha)} \int_0^x x^{\alpha-1} e^{\frac{-x}{\beta}} dx \quad (4)$$

When $t = x/\beta$, the gamma cumulative distribution function is expressed by the following formula (Yacoub and Tayfur 2020):

$$G(x) = \frac{1}{\Gamma(\alpha)} \int_0^x t^{\alpha-1} e^{-t} dt \quad (5)$$

The gamma distribution is undefined for values of $x = 0$; however, because precipitation time series may include zero values, the cumulative probability distribution H(x) is adjusted to account for both zero and non-zero precipitation values. This adjusted cumulative distribution is defined as follows (Lloyd-Hughes and Saunders 2002):

$$\mathrm{H(x) = q + (1 - q)G(x)} \quad (6)$$

Table 2 Classification of drought conditions according to the SPI (McKee et al. 1993)

SPI	Class	Symbol
≥ 2	Extremely Wet	EW
1.50 ~ 1.99	Severely Wet	SW
1.00 ~ 1.49	Moderately Wet	MoW
0.99 ~ 0	Mildly Wet	MW
0 ~ −0.99	Mildly Drought	MD
−1.00 ~ −1.49	Moderate Drought	MoD
−1.50 ~ −1.99	Severe Drought	SD
≤—2	Extreme Drought	ED

Here, q represents the probability of zero precipitation. If m denotes the number of zero-precipitation occurrences in the time series, then q can be estimated as $q = m/n$. The cumulative probability function (*x*) is then transformed into the SPI, which follows a standard normal distribution with a mean of zero and a variance of one. The SPI value corresponding to the computed (*x*) is obtained using the following approximation formulas (Abramowitz and Stegun 1965):

$$0 < \mathrm{H(x)} < 0.5, \mathrm{SPI} = -\left(\mathrm{t} - \frac{\mathrm{c_0 + c_1 t + c_2 t^2}}{\mathrm{1 + d_1 t + d_2 t^2 + d_3 t^3}}\right), \mathrm{t} = \sqrt{\ln\left(\frac{1}{(\mathrm{H(x)})^2}\right)} \quad (7)$$

$$0.5 < \mathrm{H(x)} < 1.0, \mathrm{SPI} = +\left(\mathrm{t} - \frac{\mathrm{c_0 + c_1 t + c_2 t^2}}{\mathrm{1 + d_1 t + d_2 t^2 + d_3 t^3}}\right), \mathrm{t} = \sqrt{\ln\left(\frac{1}{(1.0 - \mathrm{H(x)})^2}\right)} \quad (8)$$

In this equation, the constants are defined as follows: $c_0 = 2.515517$, $c_1 = 0.802853$, $c_2 = 0.010328$, $d_1 = 1.432788$, $d_2 = 0.189269$ and $d_3 = 0.001308$ (McKee et al. 1995). The normalization of SPI values ensures that both dry and wet periods are represented consistently across the selected time scale. A drought event is identified when the SPI value falls below −1, marking the onset of drought. The duration during which the index remains below −1 is considered the drought period (McKee et al. 1995; Mishra and Desai 2005; Mishra and Singh 2011). Based on the SPI values, drought severity categories are presented in Table 2 (McKee et al. 1993).

As the value of SPI decreases from zero to negative, the intensity of drought increases. Conversely, as SPI increases from zero to positive, the intensity of precipitation rises.

Results

In this study, drought analysis was performed with SPI by using the estimated precipitation values generated as a result of climate projections (HadGEM2-ES RCP4.5 and HadGEM2-ES RCP8.5) for the period 2023–2080 of Tokat, Çorum, Amasya, Ordu, and Samsun meteorological stations, which have sufficient observation length in the Central Black Sea region. The SPI was applied at four different time scales (1 month, 3 months, 6 months, and 12 months) for five stations. SPI diagrams estimated according to the HadGEM2-ES RCP4.5 (Scenario 1) and HadGEM2-ES RCP8.5 (Scenario 2) climate models of Tokat, Çorum, Amasya, Ordu, and Samsun are presented in Figs. 2, 3, 4, 5 and 6, respectively. The number of repetitions of humid/drought periods within the scope of the scenarios are given in Tables 3, 4, 5, 6 and 7, respectively. As in Fig. 7, the annual precipitation for the 2023–2080 period is presented according to two distinct scenarios: RCP4.5 and RCP8.5, as defined by the HadGEM2-ES climate model. Moreover, Tables 8, 9, 10, 11 and 12 present the changes between the projected future drought conditions (2023–2080) as estimated under the specified scenarios and the drought conditions that were determined from 1971–2022.

When the results in Fig. 2 and Table 3 for Tokat were evaluated together(RCP4.5), SPI-1 results show that although there was a SD period in January 2023, EW periods were determined in 2023 and 2025. In July 2025, it was

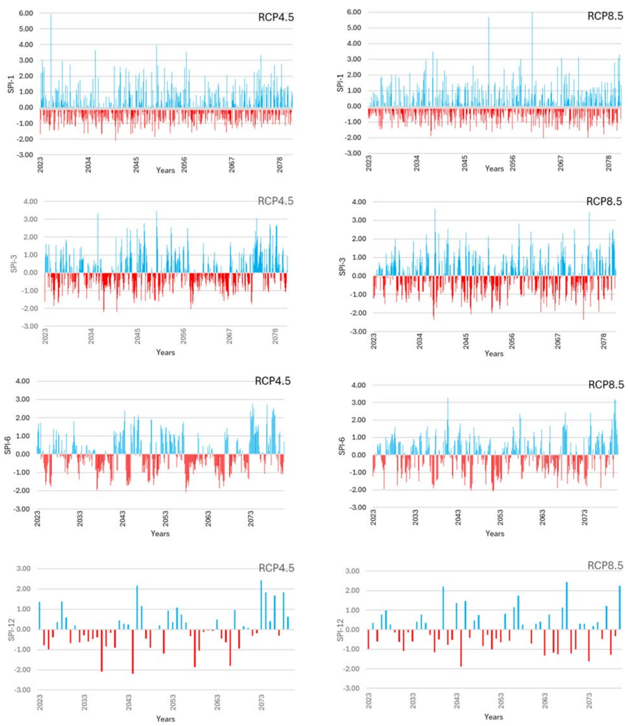

Fig. 2 Temporal distribution of SPI results for Tokat

EW with an index of 5.89 and this value was the maximum. EW periods became more frequent between 2040–2057 and 2072–2078. There are severe and ED periods in 2023, 2033, 2034, 2037, 2040, 2043–2044, 2049, 2052, 2057, and 2065. The period between 2058 and 2071 was generally considered MW and MD. SPI-3 results show ED periods in 2037, 2040, and 2057, and in 2049, both SD and EW periods were identified in the same year pattern. It can be stated that EW periods will be entered consecutively in 2073, 2076, and 2078. SPI-6 results show SD in 2025–2026, 2037, 2040, 2044, 2049–2050, 2057–2058, 2065–2066. In 2073 and 2078, consecutive EW periods were calculated in six-month sequences in the same year. In the SPI-12 results, 2037 and 2044 are ED years, while 2045 and 2073 are EW years.

When the results of Scenario 2(RCP8.5) in Fig. 2 and Table 3 for Tokat are evaluated together, SPI-1 results show that SD and ED periods are not expected until 2036. After 2037, SD have been determined in 5–10-year periods. ED are calculated in 2063 and 2073. It was calculated that EW periods will intensify in 2066, 2067, and 2068. In SPI-3, ED periods were calculated in 2037, 2046, 2051, and 2073. 2037 and 2074 are the most SW periods. In 2079 and 2080, SW and EW periods became more frequent. When SPI-6 results are analyzed, long-term severe and ED periods were estimated in 2037, 2046, and 2051. In the years 2057, 2068, 2074, and 2079–2080, EW periods intensify. In SPI-12 results, 2040, 2068, and 2080 stand out as EW years, while 2044, and 2073 stand out as SD years.

When the results in Fig. 3 and Table 4 for Çorum were evaluated together(RCP4.5), SPI-1 results show that the periods 2041–2043, 2045–2046, and 2073–2076 are characterized by successive EW periods, while there are SD periods in 2026, 2033, 2037, 2040, and 2049. SPI-3 results show ED periods in 2037 and 2068. 2041–2043, 2045, and 2049 are EW periods. By 2073, most of the three-month translational periods throughout the year are also EW. Between 2059 and 2067, MW periods were generally determined. SPI-6 results show MoW in the 2023–2036 period. 2042–2043 was determined as EW, while 2044 was determined as SD. SD periods in 2072 were followed by SW and EW periods in 2073 and 2074. SPI-12 results show SD in 2037, 2058, and 2072, and SW and EW in 2031, 2073, and 2074.

When the results in Fig. 3 and Table 4 for Corum were evaluated together(RCP8.5), SPI-1 results show SD periods after 2037. Between 2062 and 2074, EW periods intensify. SPI-3 results show EW periods in 2027, 2038, 2040, 2043, 2059–2060, 2067–2068, 2074, and 2079. In 2037, 2053, and 2066, ED periods were determined. SPI-6 results show generally MW and often MD periods, except for 2053 and 2066. SPI-12 results show 2027 and 2068 as extremely humid, and 2053 and 2066 as SD.

When the results in Fig. 4 and Table 5 for Amasya were evaluated together(RCP4.5), SPI-1 results show SD in 2025, 2033, 2037, 2037, 2040, 2049, 2050, 2058, and 2068. EW periods come to the fore in the periods 2040–2045 and 2072–2079. SPI-3 results show EW periods in the periods of 2042–2046 and 2073–2078. In addition to intermittent SD periods, ED periods were determined in 2037. SPI-6 results show EW periods in 2031 and 2046. SD periods were calculated in 2026, 2044, 2050, 2057–2058, 2066, and 2072. SPI-12 results show ED in 2058, and EW in 2046 and 2073.

When the results of Scenario 2(RCP8.5) in Fig. 4 and Table 5 for Amasya were evaluated together, it was determined that SW and EW periods intensified between 2067–2076, and ED periods were determined in 2063 in the SPI-1 results. In 2050 and 2060, EW periods become more frequent. High index values were calculated during these periods. SPI-3 results show EW periods in 2027, 2035, 2038, 2040, 2043, 2045, 2047, 2055, 2059–2061, 2064, 2067–2068, 2071, 2074,2076, and 2079. ED periods were identified in 2037 and 2053. When the SPI-6 results were examined, EW periods in 2027, 2040, 2048, 2059, 2067–2068, 2076, and 2079, and SD and ED periods in 2028, 2036–2037, 2049, 2051–2053, 2065–2066, and 2076–2078 periods were calculated. SPI-12 results show SD in 2044, 2065, 2073, and 2078. 2068 was determined as EW, 2027, 2040, 2048, and 2080 as SW.

When the results in Fig. 5 and Table 6 for Ordu were evaluated together(RCP4.5), SD periods in 2029, 2032, 2037, 2040, 2051, 2058, 2063, 2073, and 2078 and periods of EW that recur every 2 and 3 years were calculated in

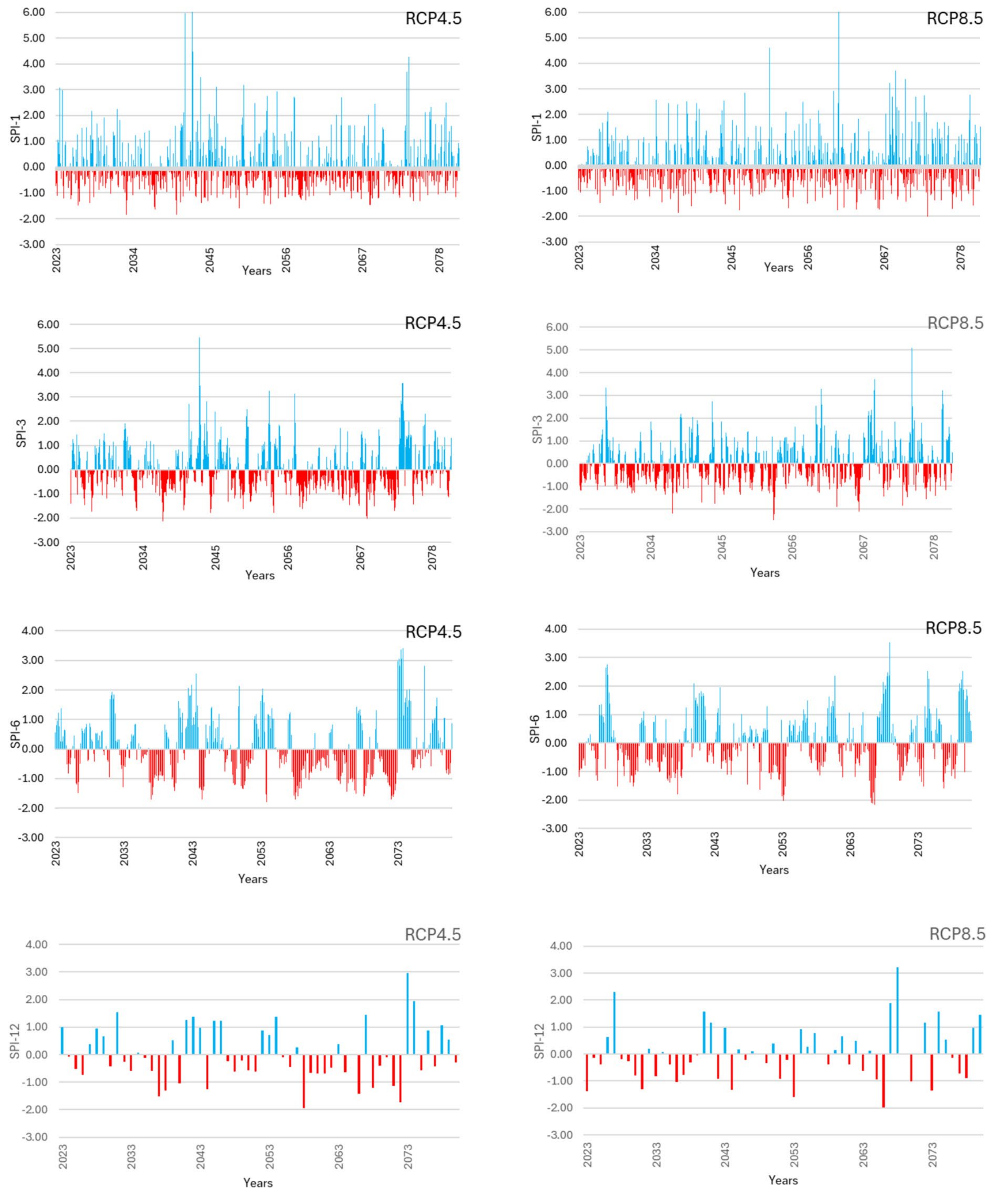

Fig. 3 Temporal distribution of SPI results for Çorum

the SPI-1 results. In 2078, SW periods intensify. Although SPI-3 results show ED periods in 2037 and 2078, the periods 2041–2049 and 2068–2079 were calculated as SW. SPI-6 results show ED periods in 2037 and 2069. EW periods were noted in the periods 2041–2049 and 2073–2078. Although ED years could not be determined in the SPI-12 results, 2032, 2037, 2048, and 2058 were calculated as SD. 2045 and 2073 were determined to be EW.

When the results in Fig. 5 and Table 6 for Ordu were evaluated together(RCP8.5), SPI-1 results show SD periods in 2029, 2040, 2044, 2063, 2065, 2070, 2073, and 2076, while EW periods in 2060 are noteworthy. Between

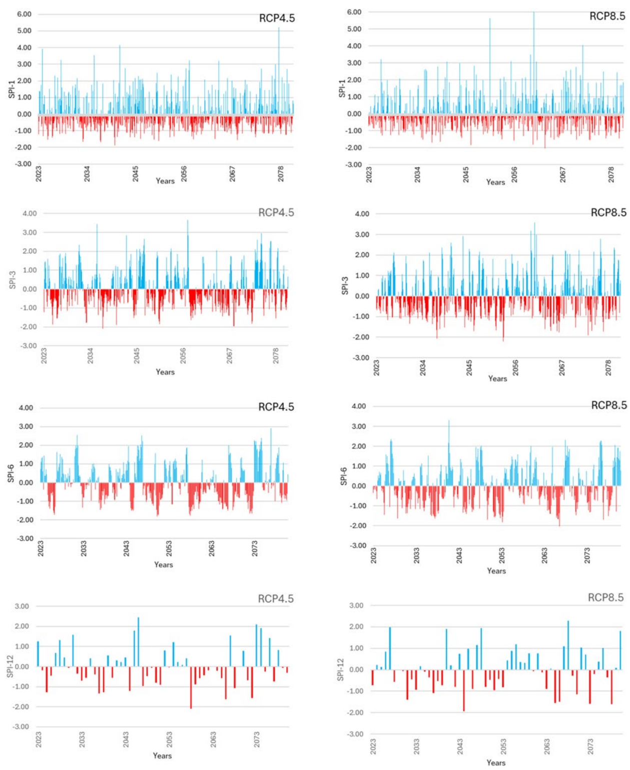

Fig. 4 Temporal distribution of SPI results for Amasya

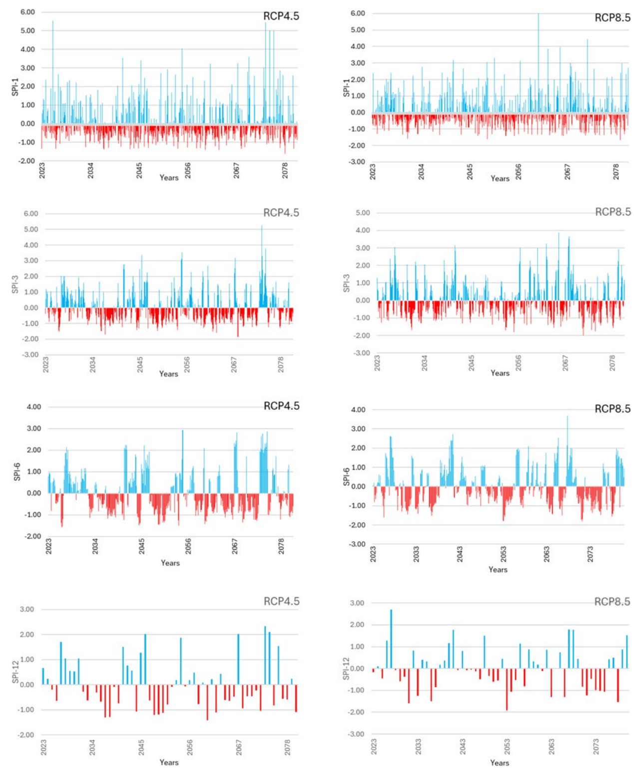

Fig. 6 Temporal distribution of SPI results for Samsun

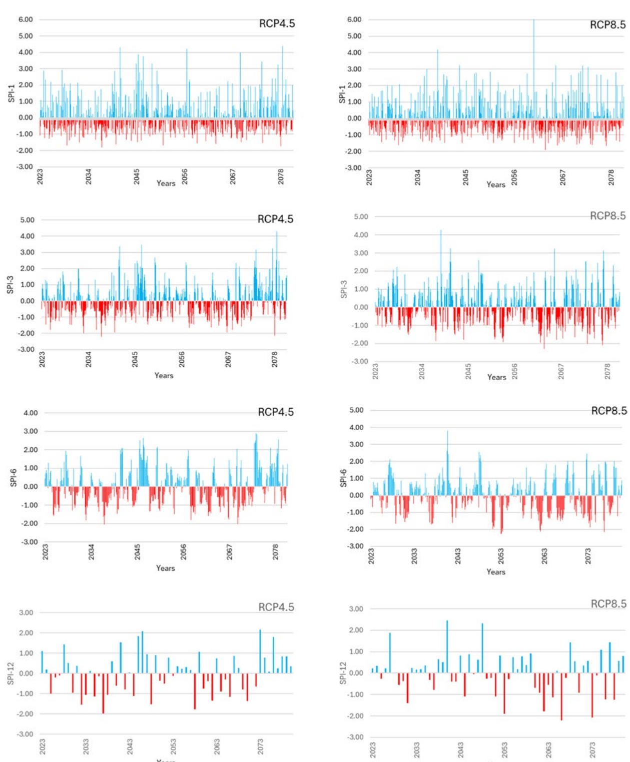

Fig. 5 Temporal distribution of SPI results for Ordu

2028 and 2079, EW periods are frequently repeated. SPI-3 results show EW periods in 2027–2028, 2038, 2040, 2047, 2065, 2068, 2070, 2072, 2075, 2077, and 2079. Long-term SD were identified in 2051, 2053, 2062, and 2076. In 2063, 2073, and 2076, ED periods were determined. SPI-6 results show EW periods in 2027, 2040, 2048, 2068, 2069, 2072, and 2079. In 2037, 2051, 2053, 2062, and 2076, SD and ED periods are intense. SPI-12 results show 2040 and 2048 as EW, and 2053, 2062, 2066, and 2073 as SD and ED.

When the results in Fig. 6 and Table 7 for Samsun were evaluated together(RCP4.5), one of the noteworthy aspects of the SPI-1 results is that between 2023 and 2080, SD periods were identified only in 2078. Another noteworthy point is the intensification of EW periods in the 2040–2061 and 2066–2079. SPI-3 results show SD in the periods 2026, 2036–2037, 2062–2063, and 2068. EW periods were calculated in 2026–2027, 2041, 2043, 2045–2046, 2054, 2057, 2059, 2061, 2067, and 2073–2074. When the SPI-6 results were analyzed, an ED period was calculated only in 2026. In the years 2041, 2067, 2073–2074, EW periods were determined during the long translation periods. While the SPI-12 results did not determine SD and ED years, 2046, 2067, and 2073–2074 were calculated as EW.

When the results in Fig. 6 and Table 7 for Samsun were evaluated together(RCP8.5), SPI-1 results showed SD in 2031,

Table 3 Drought classification results for Tokat

		EW	SW	MoW	MW	MD	MoD	SD	ED
RCP4.5	**SPI-1**	34	24	42	186	334	63	12	1
	SPI-3	21	23	50	151	254	58	19	4
	SPI-6	14	18	43	109	158	43	20	1
	SPI-12	2	3	4	17	26	2	2	2
RC P8.5	**SPI-1**	24	26	49	193	320	69	13	2
	SPI-3	15	28	52	177	216	69	18	5
	SPI-6	9	17	34	146	132	42	23	3
	SPI-12	3	1	5	19	20	8	2	0

Table 4 Drought classification results for Corum

		EW	SW	MoW	MW	MD	MoD	SD	ED
RCP4.5	**SPI-1**	30	27	40	159	366	68	6	0
	SPI-3	17	24	51	151	259	61	15	2
	SPI-6	17	24	51	151	259	61	15	2
	SPI-12	1	2	7	13	26	6	3	0
RCP.8.5	**SPI-1**	31	24	37	181	351	59	12	1
	SPI-3	23	20	51	156	256	63	7	4
	SPI-6	16	18	30	118	159	50	11	4
	SPI-12	2	3	3	18	24	6	2	0

Table 5 Drought classification results for Amasya

		EW	SW	MoW	MW	MD	MoD	SD	ED
RCP4.5	**SPI-1**	36	26	49	154	357	65	9	0
	SPI-3	22	36	40	147	262	55	17	1
	SPI-6	13	24	35	116	150	51	17	0
	SPI-12	2	4	4	15	25	5	2	1
RCP8.5	**SPI-1**	30	22	41	179	345	66	12	1
	SPI-3	27	28	40	161	243	64	14	3
	SPI-6	14	20	35	118	148	53	17	1
	SPI-12	1	4	5	17	23	4	4	0

Table 6 Drought classification results for Ordu

		EW	SW	MoW	MW	MD	MoD	SD	ED
RCP4.5	**SPI-1**	35	27	34	185	349	57	9	0
	SPI-3	28	22	35	177	239	63	14	2
	SPI-6	18	16	34	115	154	54	13	2
	SPI-12	2	3	3	23	16	7	4	0
RCP8.5	**SPI-1**	29	35	34	190	327	71	10	0
	SPI-3	17	29	45	180	221	62	23	3
	SPI-6	12	20	20	155	127	47	19	6
	SPI-12	2	1	3	24	18	6	2	2

2049, and 2079. Although MW and MD were intense, EW periods were identified every five years. SPI-3 results show SD in 2031, 2053, 2055, 2064, 2064, 2071, 2073, 2074, and 2078, while ED periods were not identified. In 2026–2027, 2030, 2032, 2034, 2038, 2041, 2056, 2058, 2060, 2062, 2065, 2067–2068, and 2079–2080, EW periods were determined. SPI-6 results show SD periods in 2025, 2025, 2053, 2071, and 2078. In 2027, 2040–2041, 2058, 2065, and 2067, EW periods were noteworthy. In the SPI-12 results, only 2027 was calculated as EW. 2031, 2053, and 2078 were in the SD class.

Table 7 Drought classification results for Samsun

		EW	SW	MoW	MW	MD	MoD	SD	ED
RCP4.5	**SPI-1**	34	22	51	136	403	49	1	0
	SPI-3	26	27	38	143	288	51	7	0
	SPI-6	25	15	25	104	189	46	2	0
	SPI-12	4	4	3	14	23	10	0	0
RCP8.5	**SPI-1**	35	26	37	161	367	67	3	0
	SPI-3	28	20	42	151	267	59	13	0
	SPI-6	13	27	30	106	170	51	9	0
	SPI-12	1	4	4	18	20	8	3	0

According to Table 8 for Tokat**,** in SPI-1 results, the MW category was calculated to increase by 2.69% in HadGEM2-ES RCP4.5 (Scenario 1) and 3.69% in HadGEM2-ES RCP8.5 (Scenario 2). According to SPI-3 results, in Scenario 1, MW decreases by 3.20%, while MD increases by 4.34%. In Scenario 2, MD decreased, while MoD increased by 1.32%. According to SPI-6 results, in Scenario 1, an increase of 2.90% in MoW, a decrease of 3.37% in MW, and a decrease of 1.13% in ED were determined. In Scenario 2, an increase of 5.74% in MW and a decrease of 7.05% in MD were calculated. In Scenario 1 of SPI-12, a decrease of 4.64% in MoD, an increase of 12.14% in MD, and a decrease of 10.01% in MoD were calculated, while in Scenario 2, an increase of 3.25% in the EW, a decrease of 4.05% in periods of SW and an increase of 3.91% in MD were determined. When the averages of monthly precipitation values were compared, while it was 36.05 mm between 1971–2022, it increased between 2023–2080 and was calculated as 48.53 mm in Scenario 1 and 49.71 mm in Scenario 2. The highest precipitation value was 141.10 mm between 1971–2022, while it increased between 2023–2080 and was calculated as 185.70 mm in Scenario 1 and 197.20 mm in Scenario 2.

In accordance with Table 9 for Corum, in SPI-1, an increase of 6.27% in MD was calculated according to Scenario 1 and an increase of 4.12% was calculated according to Scenario 2. SPI-3 results showed an increase in MD in Scenario 1, similar to SPI-1 results. SPI-6 results showed an increase of 3.10% in Scenario 1 and 4.90% in Scenario 2 in MD and MoD. SPI-12 results show an increase between 2.90% and 6.50% in the MD and MoD categories in both Scenarios. In addition, an increase was determined in the MoW category. When the average monthly precipitation values were compared, while it was 37.33 mm between 1971–2022, it decreased to 35.99 mm in Scenario 1 and increased to 38.91 mm in Scenario 2 for 2023–2080. While the highest precipitation value was 220.10 mm between 1971–2022, it was calculated as 237.9 mm in Scenario 1 and 209.60 mm in Scenario 2 for 2023–2080.

By Table 10 for Ordu, SPI-1 results showed a 10.24% increase in MD rates in Scenario 1 and a 7.08% increase in Scenario 2. SPI-3 results show an increase in MD in both scenarios, in line with SPI-1 results. SPI-6 results showed an increase of 4%–5% in MD and MoD in Scenario 1 and an increase of 3.61% in Scenario 2 in MoD. SPI-12 results show an increase between 1.5% and 5% in MoD and SD categories in both scenarios. When the averages of monthly precipitation values were compared, while it was 87.70 mm between 1971–2022, it decreased between 2023–2080 and was calculated as 72.19 mm in Scenario 1 and 72.48 mm in Scenario 2. The highest precipitation value was 267.50 mm between 1971–2022, while it increased between 2023–2080 and was calculated as 486.20 mm in Scenario 1 and 275.80 mm in Scenario 2.

In accordance with Table 11 for Amasya**,** SPI-1 results show a decrease in MW and an increase of 3.22% in Scenario 1, while it increased by 1.49% in Scenario 2. SPI-3 results show an increase in MD in both scenarios, in line with SPI-1 results. SPI-6 results show an increase in the range of 1.5% to 5.5% in MD and MoD. SPI-12 results show an increase of 1.72% in ED in Scenario 1 and an increase in SD by 4.97% in Scenario 2. On the other hand, while there was an increase in the range of 5%−8.5% in MD, a decrease in the range of 4%−7% in MoD. In addition, it was determined that SW periods increased by 4.97% in both scenarios. While the average monthly precipitation value was 37.90 mm between 1971–2022, it increased between 2023–2080 and was calculated as 38.74 mm in Scenario 1 and 41.36 mm in Scenario 2. The highest precipitation value was 153.90 mm between 1971–2022, while it increased between 2023–2080 and was calculated as 186.10 mm in Scenario 1 and 231 mm in Scenario 2.

According to Table 12 for Samsun, in Scenario 1, SPI-1 results show a decrease in MW and an increase of 10.31% in MD, while in Scenario 2 it shows an increase of 5.13%. SPI-3 results show an increase between 7 and 11% in MD in both scenarios, in line with SPI-1 results. SPI-6 results show an increase in the range of 4% to 10% in MD in both scenarios. SPI-12 results show that in Scenario 1, EW periods increased by 3.05%, SW periods by 4.97%, MD by 3.12%, and MoD by 7.63%, while MW periods decreased by 10.48%. In Scenario 2, it was determined that SW, MoD,

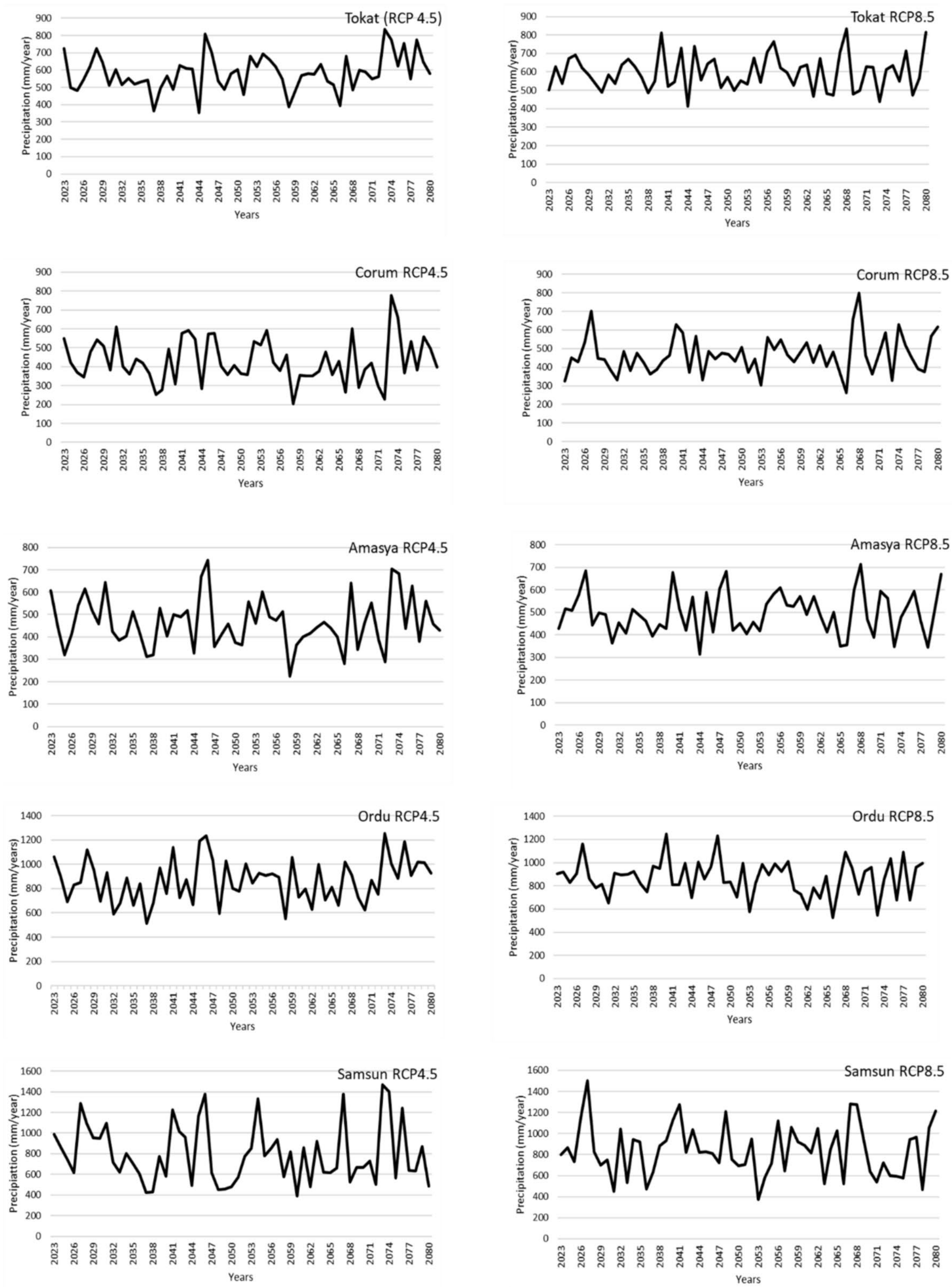

Fig. 7 Temporal distribution of Annual Precipitation for 2023–2080

and SD periods increased by 1%−5%, while MW periods decreased by 3.58%. While the average monthly precipitation value was 58.91 mm between 1971–2022, it increased between 2023–2080 and was calculated as 66.55 mm in Scenario 1 and 70.11 mm in Scenario 2. The highest precipitation value was 269.80 mm between 1971–2022, while

Table 8 Proportional changes in drought classification between 1971–2022 and 2023–2080 for Tokat

1971–2022/2023–2080		EW	SW	MoW	MW	MD	MoD	SD	ED
RCP4.5	**SPI-1**	0.88%	−2.00%	−0.54%	2.69%	0.23%	−1.04%	−0.20%	−0.02%
	SPI-3	0.54%	−1.61%	1.12%	−3.20%	4.37%	−0.58%	−1.34%	0.69%
	SPI-6	0.15%	0.04%	2.90%	−3.37%	−0.64%	2.07%	−0.02%	−1.13%
	SPI-12	1.53%	−0.60%	−4.64%	0.46%	12.14%	−10.01%	−2.32%	3.45%
RCP8.5	**SPI-1**	−0.56%	−1.71%	0.47%	3.69%	−1.78%	−0.18%	−0.06%	0.13%
	SPI-3	−0.49%	−0.75%	1.47%	1.29%	−2.18%	1.32%	−1.51%	0.86%
	SPI-6	−1.08%	−0.21%	0.68%	5.74%	−7.05%	1.83%	0.72%	−0.63%
	SPI-12	3.25%	−4.05%	−2.92%	3.91%	1.79%	0.33%	−2.32%	0.00%

Table 9 Proportional changes in drought classification between 1971–2022 and 2023–2080 for Corum

1971–2022/2023–2080		EW	SW	MoW	MW	MD	MoD	SD	ED
RCP4.5	**SPI-1**	−0.02%	−0.93%	−0.82%	−3.28%	6.27%	−0.81%	−0.42%	0.00%
	SPI-3	−0.34%	−0.29%	0.33%	−4.93%	7.16%	−0.44%	−1.26%	−0.23%
	SPI-6	−0.64%	0.29%	−0.55%	−3.64%	4.00%	3.10%	−0.71%	−1.85%
	SPI-12	−0.20%	−4.24%	8.22%	−14.12%	6.37%	6.50%	−0.60%	−1.92%
RCP8.5	**SPI-1**	0.13%	−1.36%	−1.25%	−0.12%	4.12%	−2.10%	0.44%	0.14%
	SPI-3	0.70%	−0.97%	0.33%	−4.06%	6.64%	−0.10%	−2.64%	0.11%
	SPI-6	0.37%	0.59%	−1.95%	−0.61%	−1.50%	4.90%	−0.59%	−1.21%
	SPI-12	1.53%	−2.52%	1.33%	−5.50%	2.92%	6.50%	−2.32%	−1.92%

Table 10 Proportional changes in drought classification between 1971–2022 and 2023–2080 for Ordu

1971–2022/2023–2080		EW	SW	MoW	MW	MD	MoD	SD	ED
RCP4.5	**SPI-1**	1.66%	−1.57%	−2.49%	−2.43%	10.24%	−3.99%	−1.11%	−0.32%
	SPI-3	2.52%	−1.01%	−2.04%	−5.06%	8.71%	−0.29%	−1.82%	−1.00%
	SPI-6	2.24%	−0.73%	0.13%	−7.66%	4.41%	5.33%	−1.19%	−2.53%
	SPI-12	−0.40%	3.25%	−0.60%	−4.58%	−3.18%	4.38%	4.97%	−3.85%
RCP8.5	**SPI-1**	0.80%	−0.42%	−2.49%	−1.71%	7.08%	−1.98%	−0.97%	−0.32%
	SPI-3	0.62%	0.19%	−0.32%	−4.54%	5.60%	−0.46%	−0.27%	−0.83%
	SPI-6	0.76%	0.26%	−3.32%	2.19%	−2.24%	3.61%	0.28%	−1.54%
	SPI-12	−0.40%	−0.20%	−0.60%	−2.85%	0.27%	2.65%	1.53%	−0.40%

Table 11 Proportional changes in drought classification between 1971–2022 and 2023–2080 for Amasya

1971–2022/2023–2080		EW	SW	MoW	MW	MD	MoD	SD	ED
RCP4.5	**SPI-1**	0.69%	−0.75%	1.75%	−4.80%	3.22%	−0.12%	0.01%	0.00%
	SPI-3	0.52%	2.75%	−2.91%	−4.85%	6.90%	−1.09%	−0.72%	−0.60%
	SPI-6	0.45%	2.89%	−0.17%	−8.79%	5.90%	1.57%	−0.76%	−1.10%
	SPI-12	−2.32%	4.97%	−0.80%	−8.75%	8.49%	−4.84%	1.53%	1.72%
RCP8.5	**SPI-1**	−0.18%	−1.33%	0.60%	−1.20%	1.49%	0.03%	0.44%	0.14%
	SPI-3	1.39%	1.37%	−2.91%	−2.43%	3.63%	0.46%	−1.24%	−0.25%
	SPI-6	0.70%	1.90%	−0.17%	−8.30%	5.41%	2.07%	−0.76%	−0.85%
	SPI-12	−4.05%	4.97%	0.93%	−5.31%	5.04%	−6.56%	4.97%	0.00%

Table 12 Proportional changes in drought classification between 1971–2022 and 2022–2080 for Samsun

1971–2022/2023–2080		EW	SW	MoW	MW	MD	MoD	SD	ED
RCP4.5	**SPI-1**	0.72%	−0.69%	−0.85%	−5.46%	10.31%	−2.09%	−1.94%	0.00%
	SPI-3	0.44%	1.39%	0.21%	−8.61%	10.81%	−2.17%	−1.87%	−0.19%
	SPI-6	2.31%	−0.15%	−1.81%	−5.70%	9.46%	0.07%	−3.35%	−0.82%
	SPI-12	3.05%	4.97%	−2.52%	−10.48%	3.12%	7.63%	−3.85%	−1.92%
RCP8.5	**SPI-1**	0.86%	−0.11%	−2.86%	−1.87%	5.13%	0.49%	−1.65%	0.00%
	SPI-3	0.79%	0.18%	0.90%	−7.23%	7.19%	−0.79%	−0.84%	−0.19%
	SPI-6	−0.64%	2.80%	−0.58%	−5.21%	4.78%	1.30%	−1.63%	−0.82%
	SPI-12	−2.12%	4.97%	−0.80%	−3.58%	−2.06%	4.18%	1.33%	−1.92%

it increased between 2023–2080 and was calculated as 675.10 mm in Scenario 1 and 503.10 mm in Scenario 2.

Within the scenarios used, it was concluded that from 2023 to 2080, MW periods will decrease, and MD and MoD periods will increase in the Central Black Sea Region. An increase in precipitation is expected across the region except for Ordu. The increase in drought and the increase in precipitation averages are considered to be the most concrete indicators of climate change.

Monthly average precipitation and SPI-12 values for the period 1971–2022 and the period 2023–2080 (Scenario 1 and Scenario 2) for the coastal region (Samsun and Ordu) and inland region (Tokat, Çorum, and Amasya) of the Central Black Sea Region are presented in Table 13.

As can be seen in Table 13, the average precipitation in the inland region increases by 2%−38% (except Çorum, Scenario 1). MW and MD are the dominant drought classes in the inland region according to SPI-12. These MW values decrease by 0%−41% in Scenario 1 and decrease by 16%−17% in Scenario 2 (except Tokat, Scenario 2). On the other hand, MD increases by 15%−36% in Scenario 1 and increases by 3%−14% in Scenario 2. In the coastal region, average precipitation amounts decrease by approximately 17% in Ordu, while it increases by 12%−19% in Samsun in both scenarios. MW and MD are the dominant drought classes in the coastal region according to SPI-12. In this regard, MW decreases by 9%−31% in Scenario 1 and decreases by 7%−11% in Scenario 2. While MD decreased by 10% in Ordu in Scenario 1 and increased by 8% in Samsun. According to Scenario 2, while no proportional change could be determined in Ordu, it decreased by 8% in Samsun.

Discussion

It was determined that drought events will increase with the decrease in precipitation caused by global warming (Karaman and Gökalp 2010). It is stated that Türkiye is among the countries adversely affected by climate change in the future, and desertification will occur due to the increase in temperature (Ustun 2008). According to climate projections, Altınsoy et al. (2011) determined that the Mediterranean basin and surrounding countries will be negatively affected by the consequences of climate change in the future. Precipitation is also projected to decline: by 1–10% under moderate warming and up to 30% in southern regions under

Table 13 Precipitation and SPI-12 of the Inland and Coastal regions (1971–2022 and 2023–2080)

		Monthly average precipitation (mm)			SPI-12			
		1971–2022	2023–2080 (RCP4.5)	2023–2080 (RCP8.5)	1971–2022	2023–2080 (RCP4.5)	2023–2080 (RCP8.5)	Category
Inland	Tokat	36.05	48.53	49.71	29.00%	29.00%	33.00%	MW
					33.00%	45.00%	34.00%	MD
	Corum	37.33	35.99	38.91	37.00%	22.00%	31.00%	MW
					39.00%	45.00%	41.00%	MD
	Amasya	37.9	38.74	41.36	35.00%	26.00%	29.00%	MW
					35.00%	43.00%	40.00%	MD
Coastal	Ordu	87.70	72.19	72.48	44.00%	40.00%	41.00%	MW
					31.00%	28.00%	31.00%	MD
	Samsun	58.91	66.55	70.11	35.00%	24.00%	31.00%	MW
					37.00%	40.00%	34.00%	MD

a 4 °C increase. The Black Sea Region is expected to be the least affected in terms of rainfall reduction. The National Climate Change Action Plan projects temperature increases of 2.5 °C to 5 °C across Türkiye, accompanied by risks such as drought, forest fires, water scarcity, desertification, and ecological degradation (Republic of Türkiye Ministry of Environment, Urbanization and Climate Change 2012). Within the scope of climate projections, it is predicted that temperatures will increase by 3 °C–7 °C until the 2070–2100 period, and precipitation climatology in Türkiye will vary between −0.8 mm/day and 1.2 mm/day (Turp et al. 2014). In western Türkiye, the influence of the North Atlantic Oscillation (NAO) has contributed to observed increases in sea level and temperature (Dogan et al. 2015a, b). In addition, according to another study, drought periods are predicted to prevail in the second half of the century (Yuruk 2017).

In the modeling made for the years 2016–2099 in Türkiye, it is expected that temperatures will increase. It is predicted that there will be a decrease in precipitation in the summer season, except for the west coast and northeast of the country, and a decrease in precipitation throughout the country in the autumn. Despite the predicted decreases, an increase in winter precipitation is expected (Demircan et al. 2017). By the middle of the twenty-first century, water availability in arid regions in Türkiye will decrease by 10%–30%, droughts will intensify in the south of the country and their effects will become more pronounced (Sirdas 2002; Sirdas and Sen 2003a, b). Onol et al. (2014) determined, there will be a decrease in winter precipitation of between 10 and 60%, especially in Türkiye. This is based on temperature and precipitation projections for the region, including Türkiye, made using three different global climate models (ECHAM5, CCSM3, HadCM3) and A2, A1F1 and B1 scenarios, as well as the RegCM3 Regional Climate Model for the period 2071–2099. Gürkan et al. (2016) projected climate changes in Türkiye under RCP4.5 and RCP8.5, estimating up to 2.5 °C temperature rise and significant regional decreases in precipitation, especially in Mediterranean and Fırat-Dicle basins. In the studies carried out specifically for different basins in Türkiye, it is concluded that there will be serious decreases in the average precipitation with the climate scenarios of the Akarçay Basin, which is located at the intersection of Central Anatolia, Mediterranean, and Aegean regions, and it is stated that temperatures will increase despite the decrease in precipitation (Dabanli 2017). In addition, in the 2015–2100 projections of Acısu, Selendi, Murat, Medar, Gördes, Ahmetli, Demirci, and Deliiniş sub-basins in the Gediz Basin, it is estimated that there will be long and uninterrupted wetlands in the basins until 2035, and after 2050, droughts will increase until 2080, and severe droughts will occur after 2080 (Cetin 2023).

In Anatolian geography, arid/semi-arid climate characteristics are intensely experienced. As a result of global climate change, Eastern Anatolia is expected to be the region most affected by drought in the future. Drought in Türkiye has been experienced in oscillations from the past to the present, and the effect of drought will be strengthened in climate scenarios (Ozturk 2022). Camalan et al. (2023) investigated drought trends in Central Anatolia using standardized indices and climate projection data. Findings show that drought severity has increased since 1994, with rising temperatures and irregular precipitation as key drivers. Future projections suggest further intensification of drought due to global warming. The Ministry of Environment, Urbanization and Climate Change predicts that there will be an increase in winter precipitation throughout the country and a decrease in precipitation in spring, except for the coastal/northeastern regions (Republic of Türkiye Ministry of Environment Urbanization and Climate Change 2018). The IPCC 6th Assessment Report states that global warming will cause changes in climate systems in the future. It was stated that with a warmer climate than today, very precipitous and very arid weather will come, and accordingly, floods and droughts will be experienced more frequently (IPCC 2021). In some studies, conducted in the Eastern Black Sea Region, climate change is expected to affect all settlements (Tugaç, 2022). There will be an increase in droughts and fluctuations in precipitation (Nacar et al. 2022). In addition, it was concluded that in addition to the significant increase in temperatures in the Black Sea Region, drought will gradually increase in the future (Kir 2021). In general, when the studies in the literature, including this study, are evaluated together, it is seen that there is a high probability that drought will become more widespread in Türkiye in the future, and accordingly, water shortages will occur in Türkiye.

Conclusion

This study aimed to determine the drought status of the Central Black Sea Region of Türkiye from 2023 to 2080 according to climate models. For this purpose, HadGEM2-ES RCP4.5 and HadGEM2-ES RCP8.5 scenarios for Tokat, Çorum, Amasya, Ordu, and Samsun were used. The drought situation calculated within the scope of the determined scenarios and the current situation for the 1971–2022 period were evaluated together. When the current situation in the Central Black Sea Region for 1971–2022 and the drought situation calculated by the scenarios for the 2023–2080 period were evaluated together, it was determined that the drought level will increase in the future. In addition, it was determined that normal drought periods in the interior of the region have been postponed to near-normal drought periods. It was calculated that normal drought periods were decreasing in the coastal strip of the region. However, this drought class has not been relegated to the near-normal drought class as in the inland regions. It is estimated that moderately severe drought and very humid periods will intensify in the future, especially in Samsun, while moderate/severe drought periods will be experienced frequently in Ordu.

This study is considered to be a resource to be utilized in the effective and sustainable use of water resources over the years, regional and temporal planning of agricultural product diversity, measures to be taken against natural disasters such as floods, and studies to be carried out by the state and researchers on the subject. As the continuation of this study, it is aimed to determine the severity, duration, frequency, and impact area of drought in the region by using different drought analysis methods in the literature and hydro-meteorological climate parameters within the scope of current/climate models.

Acknowledgements The meteorological data used in this manuscript were obtained from the Turkish State Meteorological Service (TSMS) for the master's thesis titled "Drought Analysis of The Central Black Sea Region Within The Scope Of Climate Projections" written by Selcuk Erdem Kurtoglu under the supervision of Asli Ulke Keskin. The authors thank the Turkish State Meteorological Service for providing the meteorological data. The authors also thank the reviewers for their constructive criticisms which have considerably improved this manuscript.

Authors contributions Selcuk Erdem Kurtoglu, Investigation, methodology, formal analysis, supervision, and writing (original draft). Aslı Ulke Keskin, Data curation, investigation, methodology, validation, supervision, and writing (original draft, review, and editing). Utku Zeybekoglu, Validation, visualization, supervision, and writing (original draft, review, and editing).

Funding Open access funding provided by the Scientific and Technological Research Council of Türkiye (TÜBİTAK).

Data availability Data will be made available on request.

Declarations

Competing interest The authors declare no competing interests.

References

Abramowitz M, Stegun IA (1965) Handbook of Mathematical Formulas, Graphs and Mathematical Tables. Dover Publications Inc, New York

Abu Arra A, Sisman E (2024a) Innovative drought classification matrix and acceptable time period for temporal drought evaluation. Water Resour Manage 38:2811–2833. https://doi.org/10.1007/s11269-024-03793-0

Abu Arra A, Sisman E (2024b) A comprehensive analysis and comparison of SPI and SPEI for spatiotemporal drought evaluation. Environ Monit Assess 196:980. https://doi.org/10.1007/s10661-024-13127-7

Abu Arra A, Alashan S, Sisman E (2024) Trends of meteorological and hydrological droughts and associated parameters using innovative approaches. J Hydrol 640:131661. https://doi.org/10.1016/j.jhydrol.2024.131661

Afshar MH, Şorman A, Tosunoğlu F, Bulut B, Yilmaz MT, Danandeh Mehr A (2020) Climate change impact assessment on mild and extreme drought events using copulas over Ankara, Turkey. Theor Appl Climatol 141:1045–1055. https://doi.org/10.1007/s00704-020-03257-6

Agyekum J, Annor T, Lamptey B, Quansah E (2018) Agyeman RYK (2018) Evaluation of CMIP5 global climate models over the volta basin: precipitation. Adv Meteoro 1:1–24. https://doi.org/10.1155/2018/4853681

Altınsoy H, Öztürk T, Türkeş M, Kurnaz ML (2011) Küresel iklim modeli kullanılarak Akdeniz Havzası'nın gelecek hava sıcaklığı ve yağış değişikliklerinin kestirilmesi. In: Proceedings of the National Geographical Congress with International Participation, 7–10 Sep. 2011, Türk Coğrafya Kurumu, İstanbul Üniversitesi (in Turkish)

Bacanli UG (2017) Trend analysis of precipitation and drought in the Aegean region, Turkey. Meteorol Appl 24:239–249. https://doi.org/10.1002/met.1622

Bacanli UG, Kargi PG (2019) Drought analysis in long and short term periods: Bursa case. J Nat Hazards Environ 5:166–174. https://doi.org/10.21324/dacd.429391

Bacanli UG, First M, Dikbas F (2009) Adaptive Neuro-Fuzzy inference system for drought forecasting. Stoch Environ Res Risk Assess 23:1143–1154. https://doi.org/10.1007/s00477-008-0288-5

Camalan G, Oguz K, Akıl S (2023) Investigation of the effect of global warming on drought conditions in the Central Anatolia Region. Disaster Sci Eng 9(1):35–55

Cetin B (2023) Performing drought analysis of basins with respect to global climate models. PhD Thesis. Manisa Celal Bayar University, Institute of Natural and Applied Sciences, Manisa (in Turkish)

Choi YW, Ahn JB, Suh MS, Cha DH, Lee DK, Hong SY, Kang HS (2016) Future changes in drought characteristics over South Korea using multi regional climate models with the standardized precipitation index. Asia-Pac J Atmos Sci 52:209–222. https://doi.org/10.1007/s13143-016-0020-1

Collins WJ, Bellouin N, Doutriaux-Boucher M, Gedney N, Hinton T, Jones CD, Liddicoat S, Martin G, O'Connor F, Rae J, Senior C, Totterdell I, Woodward S, Reichler T, Kim J (2008) Evaluation of the HadGEM2 model. Met Office Hadley Centre Technical Note no. HCTN 74, available from Met Office, FitzRoy Road, Exeter EX1 3PB. http://www.metoffice.gov.uk/publications/HCTN/index.html

Dabanli İ, Mishra AK, Sen Z (2017) Long-term spatio-temporal drought variability in Turkey. J Hydrol 552:779–792. https://doi.org/10.1016/j.jhydrol.2017.07.038

Dabanli I (2017) Climate change impact on precipitation-temperature in Turkey and drought analysis: Akarcay case study. PhD Thesis. Istanbul Technical University Science Engineering and Technology Institute, Istanbul (in Turkish)

Danandeh Mehr A, Sorman AU, Kahya E, Hesami Afshar M (2020) Climate change impacts on meteorological drought using SPI and SPEI: case study of Ankara, Turkey. Hydrological Sciences Journal 65(2):254–268. https://doi.org/10.1080/02626667.2019.1691218

Delworth TL, Broccoli AJ, Rosati A, Stouffer RJ, Balaji V, Beesley JA, Cooke WF, Dixon KW, Dunne J, Dunne KA, Durachta JW, Findell KL, Ginoux P, Gnanadesikan A, Gordon CT, Griffies SM, Gudgel R, Harrison MJ, Held IM, Hemler RS, Horowitz LW, Klein SA, Knutson TR, Kushner PJ, Langenhorst AR, Lee HC, Lin SJ, Lu J, Malyshev SL, Milly PCD, Ramaswamy V, Russell J, Schwarzkopf MD, Shevliakova E, Sirutis JJ, Spelman MJ, Stern WF, Winton M, Wittenberg AT, Wyman B, Zeng F, Zhang R (2006) GFDL's CM2 global coupled climate models. Part I: formulation and simulation characteristics. J Clim 19:643–674. https://doi.org/10.1175/JCLI3629.1

Demircan M, Arabacı H, Gurkan H, Eskioglu O, Coşkun M (2017) Türkiye İçin İklim Değişikliği Projeksiyonları, TMMOB Harita ve Kadastro Mühendisleri Odası, 16. Türkiye Harita Bilimsel ve Teknik Kurultayı, 3–6 Mayıs 2017, Ankara (in Turkish)

Demory ME, Berthou S, Fernández J, Sørland SL, Brogli R, Roberts MJ, Beyerle U, Seddon J, Haarsma R, Schär C, Buonomo E, Christensen OB, Ciarlo JM, Fealy R, Nikulin G, Peano D, Putrasahan D, Roberts CD, Senan R, Steger C, Teichmann C, Vautard R (2020) European daily precipitation according to EURO-CORDEX regional climate models (RCMs) and high-resolution global climate models (GCMs) from the High-Resolution Model Intercomparison Project (HighResMIP). Geosci Model Develop 13(11):5485–5506. https://doi.org/10.5194/gmd-13-5485-2020

Diaconescu EP, Gachon P, Laprise R, Scinocca JF (2016) Evaluation of precipitation indices over North America from various configurations of regional climate models. Atmos Ocean 54(4):418–439. https://doi.org/10.1080/07055900.2016.1185005

Dogan M, Cigizoglu HK, Sanlı DU, Ulke A (2015a) Investigation of sea level anomalies related with NAO along the west coasts of Turkey and their consistency with sea surface temperature trends. Theoret Appl Climatol 121:349–358. https://doi.org/10.1007/s00704-014-1247-3

Dogan M, Ulke A, Cigizoglu HK (2015b) Trend direction changes of Turkish temperature series in the first half of 1990s. Theoret Appl Climatol 121:23–39. https://doi.org/10.1007/s00704-014-1209-9

Duffy PB, Brando P, Asner GP, Field CB (2015) Projections of future meteorological drought and wet periods in the Amazon. Proc Natl Acad Sci USA 112(43):13172–13177. https://doi.org/10.1073/pnas.1421010112

Dunne JP, John JG, Adcroft AJ, Griffies SM, Hallberg RW, Shevliakova E, Stouffer RJ, Cooke W, Dunne KA, Harrison MJ, Krasting JP, Malyshev SL, Milly PC, Phillipps PJ, Sentman LT, Samuels BL, Spelman MJ, Winton M, Wittenberg AT, Zadeh N (2012) GFDL's ESM2 global coupled climate-carbon earth system models, Part I: Physical formulation and baseline simulation characteristics. J Climate 25:6646–6665. https://doi.org/10.1175/JCLI-D-11-00560.1

Dunne JP, John JG, Shevliakova S, Stouffer RJ, Krasting JP, Malyshev SL, Milly PC, Sentman LT, Adcroft AJ, Cooke W, Dunne KA, Griffies SM, Hallberg RW, Harrison MJ, Levy H, Wittenberg AT, Phillips PJ, Zadeh N (2013) GFDL's ESM2 global coupled climate-carbon earth system models. Part II: Carbon system formulation and baseline simulation characteristics. J Climate 26:2247–2267. https://doi.org/10.1175/JCLI-D-12-00150.1

Ekici M (2022) Türkiye's climate change policy as a public policy. PhD Thesis. Ankara Hacı Bayram Veli University, Institute of graduate Programs, Ankara (in Turkish)

Giorgetta M, Jungclaus J, Reick C, Legutke S, Brovkin V, Crueger T, Esch M, Fieg K, Glushak K, Gayler V, Haak H, Hollweg HD, Kinne S, Kornblueh L, Matei D, Mauritsen T, Mikolajewicz U, Müller W, Notz D, Raddatz T, Rast S, Roeckner E, Salzmann M, Schmidt H, Schnur R, Segschneider J, Six K, Stockhause M, Wegner J, Widmann H, Wieners KH, Claussen M, Marotzke J, Stevens B (2012) CMIP5 simulations of the Max Planck Institute for Meteorology (MPI-M) based on the MPI-ESM-MR model: The historical experiment, served by ESGF. World Data Center for Climate (WDCC) at DKRZ. https://doi.org/10.1594/WDCC/CMIP5.MXMRhi

Gürkan H, Arabacı H, Demircan M, Eskioğlu O, Şensoy S, Yazıcı B (2016) Temperature and precipitation projections based on GFDL-ESM2M using RCP4.5 and RCP8.5 scenarios for Turkey. Turk J Geographical Sci 14(2):77–88. https://doi.org/10.1501/Cogbil_0000000174

Heinrich G, Gobiet A (2012) The future of dry and wet spells in Europe: a comprehensive study based on the Ensembles regional climate models. Int J Climatol 32(13):1951–1970. https://doi.org/10.1002/joc.2421

Ilkkilic Z (2022) Analysis of the security concept in international documents on combating global climate change PhD Thesis. İstanbul University, Institute of Social Sciences, İstanbul (in Turkish)

IPCC (2021) Climate Change and Land: The Physical Science Basis. The Working Group I contribution to the Sixth Assessment Report addresses the most up-to-date physical understanding of the climate system and climate change, bringing together the latest advances in climate science. Cambridge University Press: Cambridge and New York

Karaman S, Gökalp Z (2010) Impacts of global warming and climate change over water resources. Res J Agric Sci 3(1):59–66 (in Turkish)

Kiciman A (2021) Parametrically determining the effects of seasonal climatic changes on soil erodibility factor for the geographical Central Black Sea region. MSc Thesis, Ankara University Graduate School of Natural and Applied Sciences, Ankara (in Turkish)

Kir G (2021) Evaluation of the meteorological data of the Black Sea Region using clustering analysis methods. MSc Thesis. Ondokuz Mayıs University, Graduate School of Education, Samsun (in Turkish)

Korkmaz M, Kuriqi A (2024) Regional climate change and drought dynamics in Tunceli, Turkey: Insights from drought indices. Water Conserv Sci Eng 9:49. https://doi.org/10.1007/s41101-024-00281-9

Kurtoglu SE (2024) Drought analysis of the Central Black Sea Region within the scope of climate projections. MSc Thesis, Ondokuz Mayıs University, Graduate School of Education, Samsun (in Turkish)

Lloyd-Hughes B, Saunders MA (2002) A drought climatology for Europe. Int J Climatol 22:1571–1592. https://doi.org/10.1002/joc.846

McKee TB, Doesken NJ, Kleist J (1993) The relationship of drought frequency and duration to time scales. 8th Conference on Applied Climatology, Anaheim, CA, USA, January, 179–184

McKee TB, Doesken NJ, Kleist J (1995) Drought monitoring with multiple time scales. 9th Conference on Applied Climatology, Dallas, Texas, USA, January, 233–236

Mishra AK, Desai VR (2005) Drought forecasting using stochastic models. Stoch Env Res Risk Assess 19:326–339. https://doi.org/10.1007/s00477-005-0238-4

Mishra AK, Singh VP (2011) Drought modeling - A review. J Hydrology 403:157–175. https://doi.org/10.1016/j.jhydrol.2011.03.049

Mishra AK, Singh VP (2010) A review of drought concepts. J Hydrol 391(1–2):202–216. https://doi.org/10.1016/j.jhydrol.2010.07.012

Mo KC, Lyon B (2015) Global meteorological drought prediction using the North American multi-model ensemble. J Hydrometeorol 16(3):1409–1424. https://doi.org/10.1175/JHM-D-14-0192.1

Montes-Vega MJ, Guardiola-Albert C, Rodríguez-Rodríguez M (2023) Calculation of the SPI, SPEI, and GRDI Indices for Historical Climatic Data from Doñana National Park: Forecasting Climatic Series (2030–2059) Using Two Climatic Scenarios RCP 4.5 and RCP 8.5 by IPCC. Water 15(13):2369. https://doi.org/10.3390/w15132369

Moutia S, Sinan M (2024) Drought projection from CMIP6 Climate models over Morocco in the 21st century using the Standardized Precipitation Evapotranspiration Index (SPEI). In E3S Web of Conferences,489. EDP Sciences. https://doi.org/10.1051/e3sconf/202448904003
Nacar S, San M, Kankal M, Okkan U (2022) Trend analysis of meteorological droughts for different climate change scenarios in Eastern Black Sea Region. J Inst Sci Technol 12(2):843–856 (in Turkish)
Nuri Balov M, Altunkaynak A (2020) Spatio-temporal evaluation of various global circulation models in terms of projection of different meteorological drought indices. Environ Earth Sci 79(6):126. https://doi.org/10.1007/s12665-020-8881-0
Onol B, Bozkurt D, Turunçoğlu UU, Şen ÖL, Dalfes HN (2014) Evaluation of the twenty-first century RCM simulations driven by multiple GCMs over the Eastern Mediterranean-Black Sea region. Clim Dyn 42:1949–1965. https://doi.org/10.1007/s00382-013-1966-7
Ozturk YD (2022) SPI and artificial intelligence-based analysis of drought conditions in the Black Sea region. MSc Thesis. Gümüşhane University Graduate Education Institute, Gümüşhane (in Turkish)
Rayhan Md, Afroz R (2024) Evaluating climate models to analyze drought conditions in the western region of Bangladesh. Progress Disaster Sci 23:100356. https://doi.org/10.1016/j.pdisas.2024.100356
Republic of Türkiye The Ministry of Environment, Urbanization and Climate Change (2012) İklim Değişikliği Eylem Planı 2011–2023 (in Turkish).https://webdosya.csb.gov.tr/db/iklim/banner/banner591.pdf
Republic of Türkiye The Ministry of Environment, Urbanization and Climate Change (2018) Çevre, Şehircilik ve İklim Değişikliği Bakanlığı'nın Tarihçesi (in Turkish). https://csb.gov.tr/tarihcemiz-i-7012
Salimian N, Nazari S, Ahmadi A (2021) Assessment of the uncertainties of global climate models in the evaluation of standardized precipitation and runoff indices: a case study. Hydrol Sci J 66(9):1419–1436. https://doi.org/10.1080/02626667.2021.1937178
Secci D, Tanda MG, D'Oria M, Todaro V, Fagandini C (2021) Impacts of climate change on groundwater droughts by means of standardized indices and regional climate models. J Hydrol 603:127154. https://doi.org/10.1016/j.jhydrol.2021.127154
Sen Z, Sisman E (2024) Probabilistic standardization index adjustment for standardized precipitation index (SPI). Theor Appl Climatol 155:2747–2756. https://doi.org/10.1007/s00704-023-04784-8
Sienz F, Bothe O, Fraedrich K (2012) Monitoring and quantifying future climate projections of dryness and wetness extremes: SPI bias. Hydrol Earth Syst Sci 16(7):2143–2157. https://doi.org/10.5194/hess-16-2143-2012
Sirdas S, Sen Z (2003a) Meteorological drought modelling and application to Turkey. İtüdergisi/d 2(2):95–103 (in Turkish)
Sirdas S, Sen Z (2003b) Spatio-temporal drought analysis in the Trakya region, Turkey. Hydrological Sci J 48(5):809–820. https://doi.org/10.1623/hysj.48.5.809.51458
Sirdas S (2002) Meteorological drought modelling and application to Turkey. MSc Thesis, Istanbul Technical University Science Engineering and Technology Institute, Istanbul (in Turkish)
Stagge J, Tallaksen L, Rizzi J (2015) Future meteorological drought: projections of regional climate models for Europe. In EGU General Assembly Conference Abstracts, 17
Taylan ED (2024) An approach for future droughts in Northwest Türkiye: SPI and LSTM methods. Sustainability 16(16):6905. https://doi.org/10.3390/su16166905
Thom HCS (1958) A Note on the gamma distribution. Mon Weather Rev 86(4):117–122. https://doi.org/10.1175/1520-0493(1958)086%3c0117:ANOTGD%3e2.0.CO;2
TSMS (2015) Yeni Senaryolar İle Türkiye İklim Projeksiyonlari Ve İklim Değişikliği TR2015-CC (Turkey Climate Projections and Climate Change with New Scenarios TR2015-CC). Ankara, Türkiye (in Turkish)
Tugaç Ç (2022) Climate change crisis and cities. Çevre Şehir Ve İklim Dergisi 1(1):38–60 (in Turkish)
Turkes M (2020) Impacts of climate change on food security and agricultural production: a scientific review. Aegean Geographical Journal 29(1):125–149 (in Turkish)
Turkes M (2022) What does the intergovernmental panel on climate Change's (IPCC) recently released climate change impacts, adaptation and vulnerability report tell us? Resilience 6(1):197–207. https://doi.org/10.32569/resilience.1098946. (in Turkish)
Turp MT, Ozturk T, Turkes M, Kurnaz ML (2014) Investigation of projected changes for near future air temperature and precipitation climatology of turkey and surrounding regions by using the regional climate model RegCM435. Aegean Geographical J 23(1):1–24 (in Turkish)
UNFCCC (1992) United nations framework convention on climate change. UN
Ustun HG (2008) Climate change effects on water resources. Suleyman Demirel University Graduate School of Natural and Applied Sciences. Master Thesis, Isparta, Türkiye (in Turkish)
Wood RR, Lehner F, Pendergrass AG, Schlunegger S (2021) Changes in precipitation variability across time scales in multiple global climate model large ensembles. Environ Res Lett 16(8):084022. https://doi.org/10.1088/1748-9326/ac10dd
Xu F, Bento VA, Qu Y, Wang Q (2023) Projections of global drought and their climate drivers using CMIP6 global climate models. Water 15(12):2272. https://doi.org/10.3390/w15122272
Yacoub E, Tayfur G (2017) Evaluation and assessment of meteorological drought by different methods in Trarza Region, Mauritania. Water Res Manage 31:825–845. https://doi.org/10.1007/s11269-016-1510-8
Yacoub E, Tayfur G (2020) Spatial and temporal of variation of meteorological drought and precipitation trend analysis over whole Mauritania. J African Earth Sci 163:1–12. https://doi.org/10.1016/j.jafrearsci.2020.103761
Yildirim M, Gurkan H (2016) Türkiye İçin İklim Değişikliği Projeksiyonlari. Uluslararası Katılımlı 2. İklim Değişimi ve Tarım Etkileşimi Çalıştayı, 08–09 Kasım 2016, Şanlıurfa, Türkiye (in Turkish)
Yuruk C (2017) COSMO-CLM (CCLM) climate simulations over Turkey: Performance evaluation and climate projections for the 21st century. MSc Thesis, Istanbul Technical University Science Engineering and Technology Institute, Istanbul (in Turkish)